

Measurement of the low-field anomaly in the rf surface impedance of cadmium

R. G. Goodrich

Department of Physics and Astronomy, Louisiana State University, Baton Rouge, Louisiana 70803

(Received 4 August 1980)

Measurements of the rf surface impedance of thin plates of cadmium as a function of magnetic field in low fields (0–100 G) indicate that two previously proposed mechanisms which cause a peak near zero field to be observed are operative in this case. The main intensity of the peak is caused by the length of specularly reflected skipping orbit trajectories matching the electron mean free path as proposed by Sibbald *et al.* Secondary structure on the high-field side of the peak is due to the electrons experiencing a critical scattering angle with the surface at which the surface scattering changes from specular to diffuse as proposed by Juras. Measurements of the frequency dependence of the field positions of the low-field structure and the radio-frequency size-effect linewidths support the existence of these two mechanisms being effective in this case.

When the surface of a high-purity metal is subjected to a radio frequency (rf) electric field, and the impedance of this metal is monitored as a function of an applied external magnetic field, it is found that as the externally applied magnetic field is decreased to zero the surface impedance of the metal exhibits an anomalous behavior near zero field.^{1–8} In particular, the rf impedance of metals in such an experiment exhibits a peak with decreasing magnetic field rather than a smooth change. This peak has been observed in many metals and several theories of the mechanisms causing the peak have been published.^{1–4,9} In a recent paper Gordon⁸ has concluded that the only explanation of the detailed radio-frequency and temperature dependence of his measurements on molybdenum is that due to Sibbald, Mears, and Koch¹ (SMK).

According to SMK the peak arises from skipping orbit trajectories of specularly reflected electrons contributing to the surface impedance. At sufficiently low values of the magnetic field the trajectory length of these electrons becomes equal to their mean free paths and they become ineffective in carrying current—hence, the low-field extremum. Since the trajectories of these electrons are well within the skin depth, the peak position should be frequency independent. The peak position should, however, be temperature dependent since it depends on the electronic mean free path. Detailed agreement with the frequency independence and the predicted temperature dependence have been ob-

tained for measurements on copper by SMK and on molybdenum by Gordon. It has been pointed out,² however, that the low-field anomaly still exists in samples in which no skipping orbits are observed in microwave measurements at higher magnetic fields. Another effect must be occurring which causes this discrepancy in observed data.

In 1970, Juras⁹ pointed out that a critical angle between an electron's velocity direction and the sample surface should exist at which the scattering experienced by the electron at the surface would change from specular to diffuse. This critical angle would depend on the smoothness of the surface, varying from zero for a very rough surface to $\pi/2$ for a perfectly smooth surface. As a magnetic field is increased on electrons in skipping orbit trajectories, their angle of the incidence with the surface continuously increases as their real-space orbit diameters decrease. Juras suggested that a peak in the surface impedance should be observed when the field was such that the critical angle of incidence was reached.

If the critical angle exists, the changeover from specular to diffuse scattering would cause a change in the slope of the real part of the surface impedance as a function of applied magnetic field at a field value H_δ , given by the expression

$$2 \left(\frac{H_\delta}{H_d} \right) \left(\frac{\delta}{d} \right) = 1 - \cos\theta_0, \quad (1)$$

where d is the plate thickness, δ is the effective skin depth,¹⁰ H_d is the critical-field value at which the electron trajectories span the plate thickness exactly,

$$H_d = 2 \left[\frac{c \hbar}{e} \right] \frac{k_F}{d}, \quad (2)$$

and Θ_0 is the critical angle of incidence. These expressions are specifically formulated for the radio-frequency size effect (RFSE) since all of the quantities, H_δ , H_d , d , and δ can be determined directly from this experiment. The effective skin depth δ can be determined from the RFSE linewidth¹⁰ through the relation $\Delta H / H_d = 2\delta/d$, where ΔH is the field change between the onset of the RFSE line at H_d and the first extremum in the impedance following H_d .

In addition to the low-field specular reflection effects on the surface impedance, R , Juras¹¹ also has calculated the effect of specular reflection on the RFSE line shapes. Measurements of these effects in cadmium have been reported previously.¹² In the present study the low-field anomaly is examined in cadmium under surface conditions such that the RFSE line at high fields shows no effects of specular reflection.

Cadmium was selected for this study since a low-field anomaly in the impedance exists in Cd,¹³ long-mean-free-path samples are available, the Fermi surface (FS) is well known, and with H applied parallel to the $[10\bar{1}0]$ axis in the $(11\bar{2}0)$ plane there is only one prominent RFSE line observed. The orbits giving rise to the single RFSE line for this orientation are on the third-band electron sheet (lens) of the FS of Cd. For this field crystallographic-axis orientation orbits on the second-band surface are open in the direction of the sample thickness, and the first-band orbits are ex-

tremely pointed where they enter the skin depth. Thus, only the third-band lens is expected to contribute to the skipping orbits. The real-space trajectory for these orbits in this orientation is shown in Fig. 1(b). Samples approximately 0.5 mm thick, prepared in the manner described in Ref. 12, were used for the measurements and the measuring apparatus has been described earlier.¹⁴

Recorder traces of both the low-field anomaly and the RFSE line are shown in Fig. 2. In order to obtain high precision in determining H_d and ΔH , second-derivative detection was employed. For the low-field region, the problem of obtaining accurate field measurements is twofold. The first difficulty is in accurately determining the zero-field point. This was accomplished by sweeping the field slowly through zero from negative to positive values. The rapid phase reversal at $H = 0$ produced a sharp peak under second-harmonic detection, allowing precise location of the zero-field point during a low-field sweep. The second problem is due to the fact that the low-field anomaly is rather broad. This is evident from the fact that the slope of the first-derivative curve in the neighborhood of the anomaly is relatively small. The result is that the positions of the structure cannot be determined very accurately on the basis of second-harmonic detection alone, since the second-derivative curve shows a relatively broad peak in this region. To aid in this difficulty of locating field values, a grid differentiation of the first-derivative curve was employed to locate the neighborhood of the maximum positive slope in the low-field region. This was compared to the second-derivative curve to determine the region of interest. From the second derivative then, accurate measurements of field values were made using the zero-field point as a reference from which to measure the field.

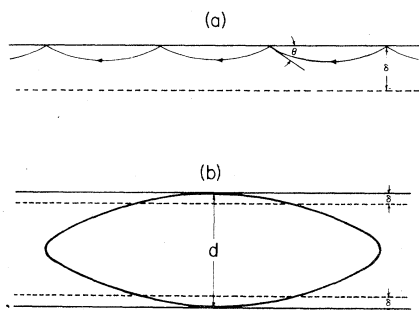


FIG. 1. (a) Skipping orbits and angle of incidence for $H < H_\delta$. H is applied along outward normal to plane of paper. (b) Real-space orbit for the lens in Cd with $\vec{H} \parallel [10\bar{1}0]$ and $H = H_d$.

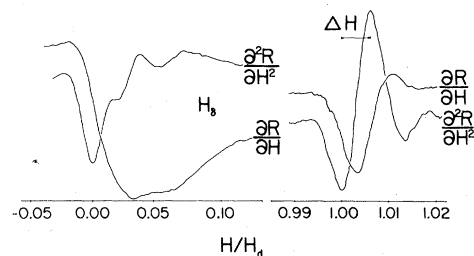


FIG. 2. Recorder tracings of $\partial R / \partial H$ and $\partial^2 R / \partial H^2$ vs H showing H_δ , H_d , and ΔH . For these tracings H is applied parallel to $[10\bar{1}0]$ and these are the only signals observed. Note the change in H/H_d scale from low to high fields. Also, the y gain at high fields is 10 greater than at low fields.

One may question at this point the prudence of arbitrarily interpreting an extremal value on second-harmonic detection output tracings as extremal points of the function itself. As is well known, the amplitude coefficient of the second harmonic term of an expansion of the output signal in terms of impressed sinusoidal modulation contains higher-order terms of all even derivatives as well as the second; thus, for broad asymmetric functions, the corresponding extremal values may be shifted with respect to one another.¹⁵ However, on the basis of the experimental evidence showing a definite shift in the peak indicated by the dotted line in Fig. 3 of the $\partial^2 R / \partial H^2$ curve as a function of frequency and the other structure on these curves being frequency independent, we feel justified in associating these points with the position of the extremal in R corresponding to the field H . The frequency-independent peak in the $\partial R / \partial H$ curve and the derivative of that peak in the $\partial^2 R / \partial H^2$ curves is due to the SMK mechanisms.

Under conditions necessary for observing the RFSE, i.e., the radio-frequency much less than the cyclotron frequency, Juras⁹ has shown that the measured critical angle θ_0 should be independent of frequency. Since under anomalous skin-effect conditions δ is proportional to $\omega^{-1/3}$, H_δ is required to be proportional to $\omega^{1/3}$. Figure 3 shows recorder tracings of the second-derivative curves at various frequencies. The vertical lines indicate extremal values which do not change, while the line through points corresponding to H_δ clearly shows a shift to higher fields with increasing radio frequency. Table I gives the measured values of H_δ , $\Delta H \propto \delta$, H_d , and the frequency-independent product as a function of frequency over almost an octave. It can be seen that the product is independent of frequency to within 1%. Plots of ω^3 vs H_δ and ΔH show the required functional dependence as described above.

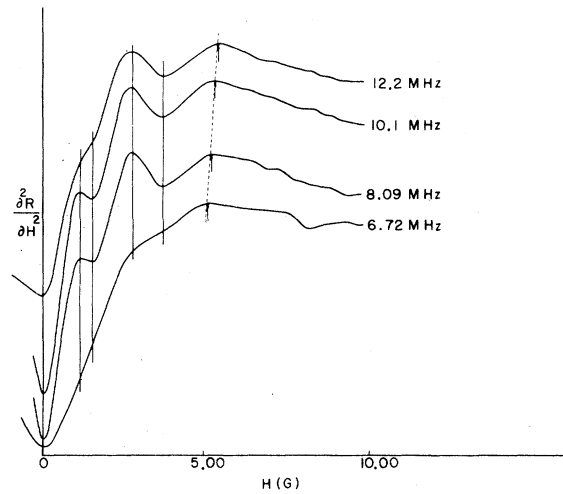


FIG. 3. Recorder tracings of $\partial^2 R / \partial H^2$ vs H showing the radio-frequency-dependent shift of the critical field H_δ . Vertical lines show the main peak structure which does not change with frequency. The loss of distinctive structure at low frequency may be due to an increased rf level which would tend to overmodulate the lines.

We note that from a semiclassical viewpoint the orbits discussed here [Fig. 1(b)] give rise to small incident angles even up to $H/H_d = 1$. Scale drawings of the stationary real-space trajectories within the sample at $H/H_d = 1$ indicate a maximum angle of incidence over most of the trajectory of approximately 0.16 rad. Since such a small critical angle, $\theta_0 = 0.04$ rad, is measured, one is led to the conclusion that the sample surface was extremely rough.

Juras has calculated the expected RFSE line shapes under conditions of complete diffuse scattering and under conditions of complete specular scattering at the sample surface.¹¹ The RFSE line observed here has the shape expected for the case of

TABLE I. Measured values of H_δ , ΔH , and H_d as a function of radio frequency. Field values are in gauss, frequencies in MHz. The last column shows the frequency-invariant dimensionless product $(H_\delta/H_d)(\Delta H/H_d) = 1 - \cos\theta_0$.

f	H_δ	ΔH	H_d	$\left[\frac{H_\delta}{H_d} \right] \left[\frac{\Delta H}{H_d} \right]$
6.724	5.12 ± 0.04	0.900 ± 0.008	70.3 ± 0.3	$(9.32 \pm 0.03) \times 10^{-4}$
8.092	5.20 ± 0.04	0.880 ± 0.008	70.2 ± 0.3	$(9.29 \pm 0.03) \times 10^{-4}$
10.096	5.33 ± 0.04	0.860 ± 0.008	70.3 ± 0.3	$(9.28 \pm 0.03) \times 10^{-4}$
12.173	5.44 ± 0.04	0.847 ± 0.008	70.3 ± 0.3	$(9.32 \pm 0.03) \times 10^{-4}$

diffuse scattering, indicating that at the fields at which the RFSE occurred the electrons were indeed being diffusely scattered. In order to check this result, samples with much smoother surfaces were prepared.¹⁶ The result of measurements on these samples is shown in Fig. 4. In this case, the surface impedance is found to change smoothly from the low-field peak to H_d with no detectable H_δ . The RFSE line shapes observed in this case are much different from the rough-surface line shapes and agree with Juras's predictions for specular reflection. The relative intensity of the SMK anomaly to the RFSE line intensity in this case is much higher than in the rough-surface case, which indicates that more of the electrons are being specularly reflected at low fields as expected. The line shape in the smooth-surface case does not change with temperature, which is in agreement with Juras's prediction.

The main portion of the low-field anomaly in cadmium shows the frequency independence predicted by SMK and appears to be due to the mean free path of electrons matching the skipping orbit trajectory length. If one assumes that the main contribution to the peak in cadmium for the present sample-field orientation is from electrons on the third-band lens, the mean free path can be calculated from the expression given by SMK:

$$l \approx \left(\frac{h}{e} \right)^{2/3} \frac{K^{1/3}}{H_0^{2/3}}$$

In this expression K is the radius of curvature of the Fermi surface, H_0 is the field position of the peak, h is Planck's constant, and e is the electronic charge. The radius of curvature of the lens in cadmium is well known.¹² From the SMK expressions, one obtains a mean free path of ~ 0.3 mm. This value is

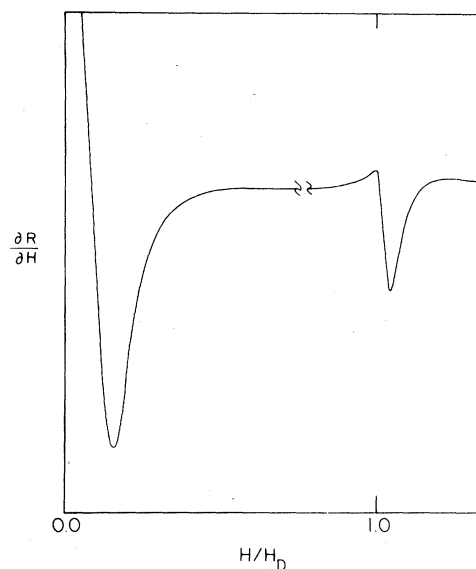


FIG. 4. Recorder tracing of $\partial R / \partial H$ vs H showing the specular reflection line shape of the RFSE line and the lack of additional structure in the SMK peak.

consistent with the fact that the RFSE line is weak in a 0.5-mm-thick sample.

In conclusion, the main contribution to the low-field anomaly in metals appears to be due to skipping orbit trajectory lengths matching the mean-free-path lengths. On samples with nonsmooth surfaces, additional effects due to a change from specular to diffuse scattering at the surface needs to be taken into account.

This work was supported in part by the National Science Foundation under Grant No. DMR 80-09826.

¹K. E. Sibbald, A. L. Mears, and J. F. Koch, Phys. Rev. Lett. **27**, 14 (1971).

²S. Pal and D. S. Falk, Phys. Rev. B **18**, 5309 (1978); V. F. Gantmakher, L. A. Falkovskii, and V. S. Tsoi, Pis'ma Zh. Eksp. Teor. Fiz. **9**, 246 (1969) [JETP Lett. **9**, 144 (1969)].

³V. S. Tsoi, Zh. Eksp. Teor. Fiz. **64**, 214 (1973) [Sov. Phys. — JETP **37**, 1078 (1973)]; B. E. Meierovich, *ibid.* **59**, 276 (1970) [*ibid.* **31**, 149 (1971)].

⁴H. D. Drew, Phys. Rev. B **5**, 360 (1972).

⁵W. M. MacInnes, B. Collet, P. A. Probst, and R.

Huguenin, J. Phys. F **7**, 655 (1977); H. H. A. Awater and J. S. Lass, *ibid.* **3**, 1113 (1973).

⁶S. A. Govorkov and V. A. Tulin, Zh. Eksp. Teor. Fiz. **70**, 1044 (1976) [Sov. Phys. — JETP **43**, 545 (1976)]; V. F. Gantmakher and Yu. V. Sharvin, *ibid.* **39**, 512 (1960) [*ibid.* **12**, 358 (1961)].

⁷J. F. Cochran and C. A. Shiffman, Phys. Rev. **140**, A1678 (1965).

⁸R. A. Gordon, Phys. Rev. B **22**, 1119 (1980).

⁹G. E. Juras, Phys. Rev. Lett. **24**, 390 (1970).

¹⁰G. E. Juras, Phys. Rev. **187**, 784 (1969).

¹¹G. E. Juras, Phys. Rev. B 2, 2869 (1970).

¹²D. A. Boudreaux and R. G. Goodrich, Phys. Rev. B 3, 3086 (1971).

¹³R. C. Jones, R. G. Goodrich, and L. M. Falicov, Phys. Rev. 174, 672 (1968).

¹⁴O. L. Steenhaut and R. G. Goodrich, Phys. Rev. B 1, 4511 (1969).

¹⁵Under the conditions where the modulation amplitude h is less than the width of the variation in R :

$$R(H + h \sin \omega t) = \left[R(H) + \frac{h^2}{4} \frac{\partial^2 R}{\partial H^2} + \frac{h^4}{16} \frac{\partial^4 R}{\partial H^4} + \frac{h^6}{1152} \frac{\partial^6 R}{\partial H^6} + \dots \right] \\ + \left[h \frac{\partial R}{\partial H} + \frac{h^3}{8} \frac{\partial^3 R}{\partial H^3} + \frac{h^5}{192} \frac{\partial^5 R}{\partial H^5} + \dots \right] \sin \omega t \\ - \left[\frac{h^2}{4} \frac{\partial^2 R}{\partial H^2} + \frac{h^4}{48} \frac{\partial^4 R}{\partial H^4} + \frac{h^6}{1536} \frac{\partial^6 R}{\partial H^6} + \dots \right] \cos 2\omega t + \dots,$$

where ω is the modulation frequency. In the present case the amplitude of the signal phase detected at ω in the neighborhood of H_δ is of order h times the signal phase detected at 2ω . This leads us to believe that R is smoothly varying in the vicinity of H_δ and that there is less than 1% error in associating the coefficients of the first- and second-harmonic terms with the first and

second derivatives of the impedance.

¹⁶The author is indebted to Professor Ray E. Ferrel of the Department of Geology at LSU for making scanning electron microscope photomicrographs of these samples. Although no quantitative data of surface roughness were obtained, the latter samples showed much less pitting under a 1000 \times magnification.